

Photoabsorption analysis of metal nanoparticles by hybrid quantum/classical scheme

Bashir Fotouhi*

Faculty of Electrical and Computer Engineering, University of Kurdistan, Kurdistan, Iran

(Received 22 March 2022; Revised 23 April 2022)

©Tianjin University of Technology 2022

The hybrid quantum/classical scheme (HQCS) is used for the photoabsorption analysis of metal nanoparticles. The HQCS divides the structure of interest into quantum and classical subsystems. First, we calculate and report Lorentz parameters for gold (Au), silver (Ag), aluminum (Al), chromium (Cr), and nickel (Ni) permittivities used in the classical subsystem. Then, photoabsorption spectra were obtained from HQCS for the single nanoparticle structures with and without two sodium (Na) atoms. The Au, Ag, Al, Cr, and Ni show strong sensitivity to the presence of the atomic subsystem. This work could pave the way for how coupled plasmon modes between metal nanoparticles and atomic structures can be utilized for sensing devices.

Document code: A **Article ID:** 1673-1905(2022)09-0519-6

DOI <https://doi.org/10.1007/s11801-022-2041-6>

Photons are transformed into plasmon form as a consequence of wave-object interactions. Spatio-temporal study of these interactions can predict the viability of such a mechanism for sensing^[1]. Some well-known applications of plasmonic waves are single-molecule detection^[2], DNA sequencing^[1], particle sorting^[3], and object trapping^[4]. The surface plasmon resonance (SPR) mechanism is susceptible to the structure shape and size^[1,3]. One of the significant aspects of interest for SPR is single-molecule sensing developed in the last few years^[1-4]. However, to study the viability of SPR in single-molecule sensing, pure classical methods are invalid in this scale, and pure quantum-mechanical methods are not efficient^[5]. Recently, a hybrid quantum/classical scheme (HQCS) has been developed based on the combinations of time-domain density functional theory (TDDFT) and classical Maxwell equations^[6]. This hybrid and robust scheme was used to predict molecule sensing via plasmon coupling in silver (Ag) and gold (Au) nanoparticles^[7]. From the computing point of view, HQCS is more efficient than ab-initio calculations^[8]. However, they are accurate in the molecular scales compared to pure classical methods such as discrete dipole approximation^[9]. Atomic coordinates, electron bands, structure sizing, and Lorentz representations of permittivities are essential in HQCS calculations. Lorentz parameters of dielectric permittivities are reported for Au and Ag^[2].

In this letter, first, we calculate and report Lorentz parameters for Au, Ag, aluminum (Al), chromium (Cr), and nickel (Ni) permittivities. Then, photoabsorption properties are analyzed for a single sphere in the pres-

ence of two sodium atoms by employing HQCS as shown in Fig.1. The HQCS method divides the proposed structure into quantum and classical subsystems. The quantum subsystem is treated using TDDFT, and the classical one is treated by the finite difference time domain (FDTD) method. The subsystems are illuminated separately, but the quantum (classical) part is also affected by the classical (quantum) electrostatic potential^[2,6]. For the classical subsystem, permittivity is modeled as a linear combination of Lorentz oscillators, demonstrated as

$$\varepsilon(\omega) = \varepsilon_{\text{Re}}(\omega) + i\varepsilon_{\text{Im}}(\omega) = \varepsilon_{\infty} + \varepsilon_0 \sum_j \frac{\beta_j}{\omega_j^2 - i\omega\alpha_j - \omega^2}, \quad (1)$$

where β_j , ω_j and α_j are parameters to fit the desired model to the experimental permittivities. As desired in the current implementation of HQCS, we assume $\varepsilon_{\infty} = \varepsilon_0$ and ω is the frequency in electron-volt. Also, ε_{Re} and ε_{Im} are real and imaginary parts of permittivity, respectively. To find optimal parameters, we search the minimum value of the following equation by derivation of the right side of Eq.(2),

$$I_{\{\beta_j, \omega_j, \alpha_j\}} = \int \sqrt{A[\varepsilon_{\text{Re}}(\omega) - \varepsilon_1(\omega)]^2 + B[\varepsilon_{\text{Im}}(\omega) - \varepsilon_2(\omega)]^2} d\omega, \quad (2)$$

where ε_1 and ε_2 are real and imaginary parts of experimental permittivity, respectively. The parameters A and B are selected to obtain the best fitted Lorentz representation for each material. The experimental

* E-mail: B.Fotouhi@uok.ac.ir

permittivities for Au, Ag, Al, Ni, and Cr are reported in Refs.[10] and [11]. The fitting frequency ranges from {0.64, 0.64, 1.23, 0.64, 1} eV to {6.63, 6.59, 8.26, 6.46, 6.02} eV for {Au, Ag, Al, Cr, Ni}. Fig.2 shows experimental and fitted data for the imaginary and real parts of Al permittivity, and similar results are obtained for other materials. Tab.1 shows all the calculated Au, Ag, Al, Cr, and Ni parameters. Because of larger values of Cr permittivity and to converge Poisson equations, a larger minimum limit is chosen for ω_j . Here we apply 8 Lorentz oscillators to get an excellent fit over the selected frequency ranges for each material. The reported Lorentz parameters are essential information that should be used in future studies of metal nanostructures via HQCS. The proposed HQCS method employs the quasistatic FDTD method, which uses dipole approximation and neglects magnetic field to calculate the optical properties of the classical subsystem. Photoabsorption spectra are calculated for a metal sphere with and without Na atoms placed near the sphere edge. For the HQCS method, the system is divided into two subsystems, quantum and classical ones. For each subsystem, a real-space grid is used. We use 2 Å and 0.5 Å grids for the classical and quantum subsystems, respectively. In the quantum subsystem, atomic coordinates and their types are used. However, for the classical subsystem, permittivity represented in the linear combination of Lorentz oscillators is desired^[7]. Each subsystem is illuminated separately by an electromagnetic field from all three directions. The quantum subsystem is the Na atoms and the classical subsystem is the metal nanoparticle. For the HQCS calculations, and we use GPAW codes^[12-15]. A time step of 10 attoseconds is chosen, and simulations are done for 20 femtoseconds.

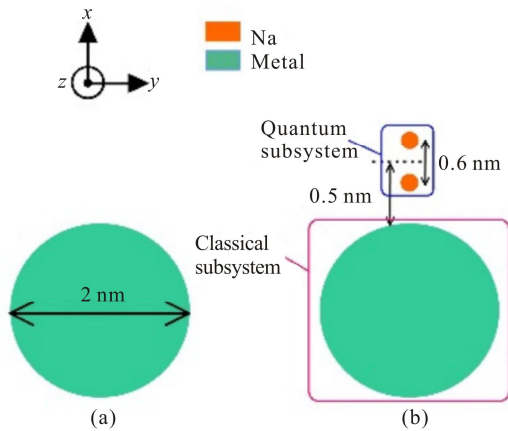


Fig.1 Schematic of (a) a nanoparticle and (b) that with two Na atoms (The Na atoms are treated as quantum and metal nanoparticles as classical subsystems, respectively. The quantum subsystem is 0.5 nm far away from the surface of the nanoparticle.)

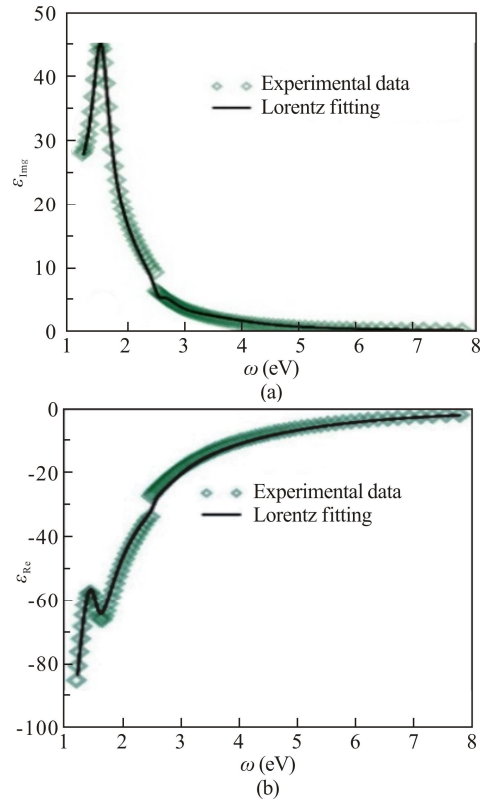


Fig.2 Comparison of experimental and Lorentz representation of relative permittivities for Al: (a) Imaginary parts of permittivity; (b) Real parts of permittivity

Tab.1 Lorentz parameters β_j (eV²), ω_j (eV) and α_j (eV) for permittivities of Au, Ag, Al, Cr and Ni

	Au	Ag	Al	Cr	Ni
β_0	90.502	22.677	18.791	19.477	11.134
ω_0	3.818	4.277	1.569	1.334	1.620
α_0	1.504	1.189	0.385	1.219	2.960
β_1	-14.840	4.006	90.187	8.939	47.906
ω_1	0.608	0.774	0.765	2.411	7.405
α_1	0.498	0.636	0.100	0.776	0.589
β_2	37.917	-23.690	17.575	-19.060	12.165
ω_2	5.654	3.003	0.101	0.368	0.776
α_2	3.000	3.000	3.000	0.100	0.769
β_3	5.894	55.874	-53.930	35.865	14.150
ω_3	2.807	5.874	1.020	3.790	0.100
α_3	0.719	3.000	0.100	3.000	0.100
β_4	98.094	95.998	12.378	38.987	31.878
ω_4	0.100	0.171	0.107	0.100	0.100
α_4	0.250	0.105	3.000	0.135	0.100
β_5	79.961	-11.860	9.034	40.122	97.719
ω_5	7.924	3.973	2.048	2.572	4.711
α_5	1.235	0.898	0.703	3.000	3.000
β_6	-22.570	15.337	67.174	34.153	66.493
ω_6	0.100	2.630	0.775	0.100	1.656
α_6	3.000	2.460	0.100	3.000	3.000
β_7	-51.400	-21.990	29.599	88.613	-7.415
ω_7	3.794	0.465	0.915	7.033	3.726
α_7	1.206	0.596	0.211	3.000	1.357

In Fig.3, photoabsorption spectra for Au, Ag, Al, Cr, and Ni, obtained from the HQCS method, are shown. Note that the photoabsorption quantity is defined as the relative absorption rate of the system compared to a classical single-electron oscillator^[16]. The photoabsorption quantities are shown on a logarithmic scale. For the results presented in Fig.3, our Lorentz parameters are used in the HQCS calculations. Generally, when there is no quantum subsystem, as presented in Fig.1(a), the HQCS results are predictable and similar to the classical calculations^[7]. For the structure presented in Fig.1(b), results presented in Fig.3 show that HQCS can predict the effect of two Na atoms on the absorption spectra. The pure classical methods have a limited frequency range, and their non-accurate results for small objects such as molecules and atoms are challenging. However, utilizing both quantum and classical representations simultaneously for a system is a powerful method to predict the optical properties of nanostructures, especially to sense molecules and atoms.

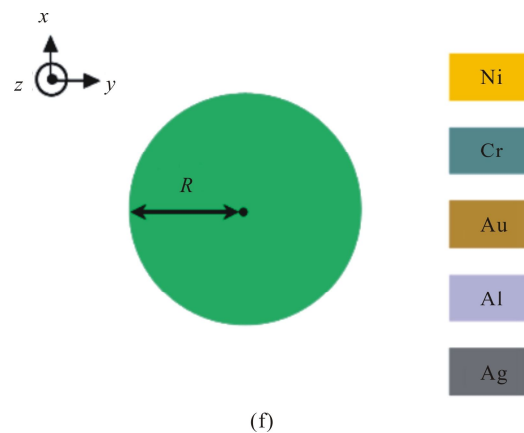
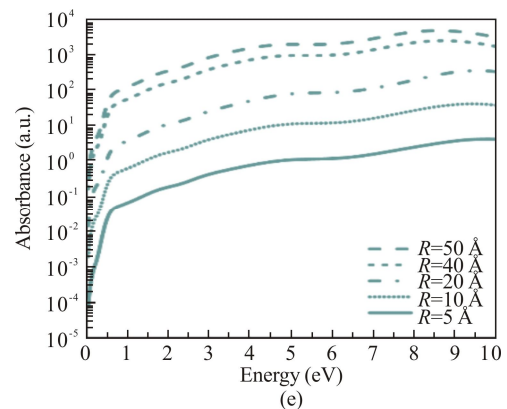
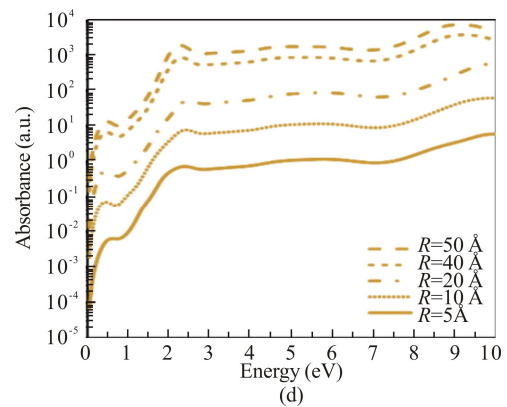
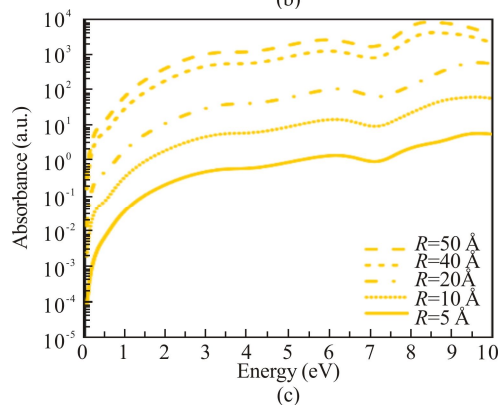
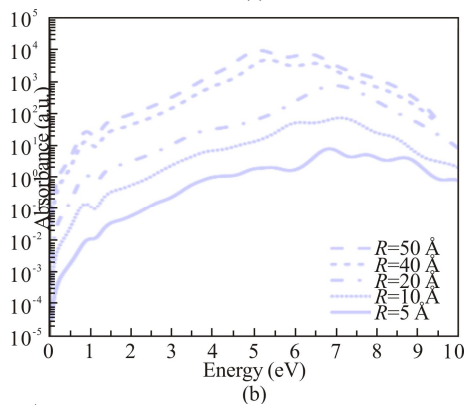
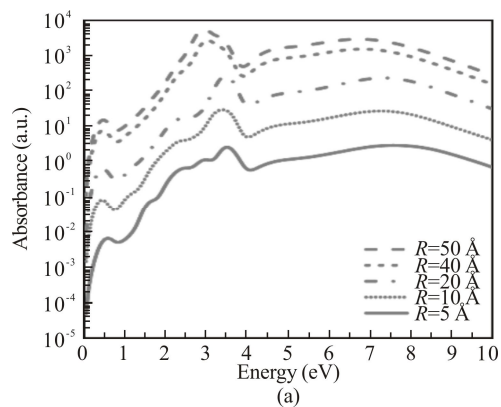


Fig.3 Photoabsorption spectra obtained from HQCS method for (a) Ag, (b) Al, (c) Ni, (d) Au, and (e) Cr nanoparticles (Effects of the size variations are shown for all nanoparticles. The photoabsorption quantities are shown on a logarithmic scale.)

Variation of the nanoparticle radius from 5 Å to 50 Å is studied for all materials. In all cases, increasing the nanoparticle radius results in more photoabsorption. Photoabsorption spectra for each material contain one or more absorption peaks. For example, Ag has one dominant peak at about 3 eV and another at 0.5 eV. The energy of the dominant peak of the photoabsorption spectrum is decreased by increasing the nanoparticle radius. The peak in the lower energy range is less sensitive to size variations. Similarly, the Au has two dominant peaks. Energy ranges for these two peaks are slightly

lower than those of silver. In none of the cases, size variation could remove the peaks or introduce a new peak to the photoabsorption spectrum. Al shows higher, and Cr shows lower photoabsorption than other metals for the same radius. As a general trend for all the metal nanoparticles, increasing the illuminated energy from 0 to 10 eV results in the increasing photoabsorption quantity.

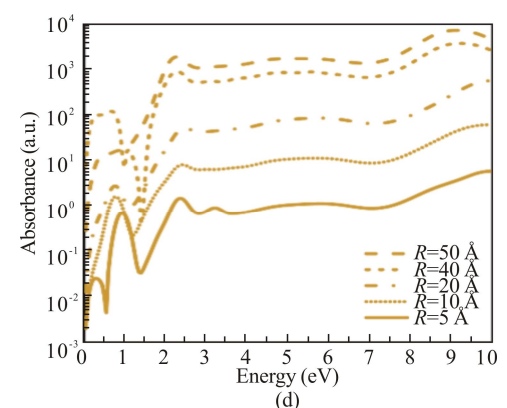
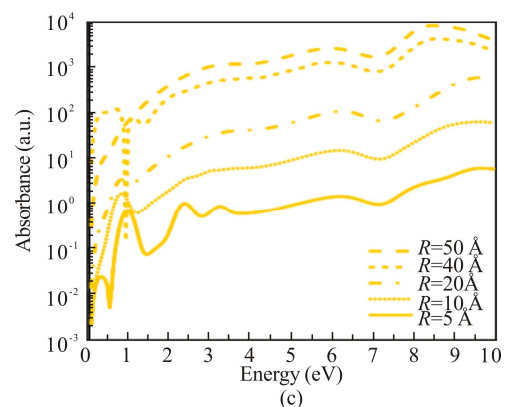
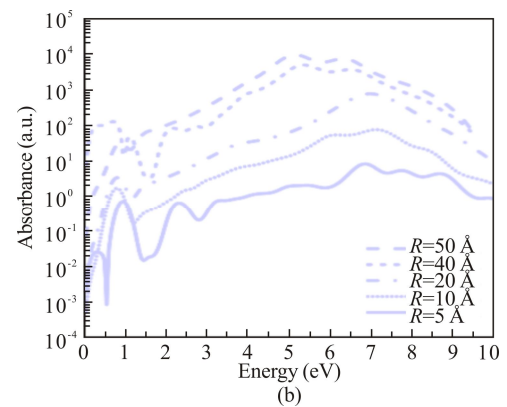
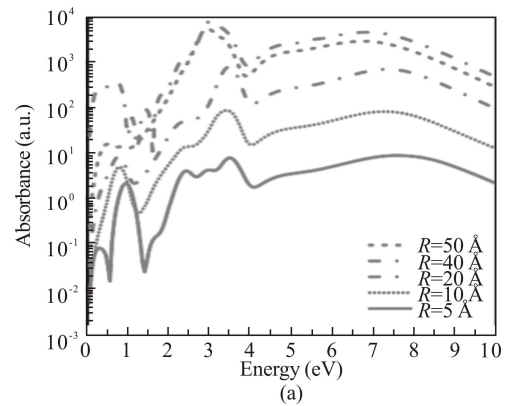
We evaluate our simulation results compared to some practical photoabsorption analyses of metal nanoparticles. The experimental investigations of a single Au nanoparticle (5 nm in diameter) show the peak absorption at 2.35 eV^[17]. Our simulation results for the same nanoparticle show the peak absorption at 2.35 eV. For the silver nanoparticle of 20 nm^[18], the practical absorption peak is about 430 nm, and our simulation results show 427 nm. Thus, our simulation results have good agreement with those experimentally performed for the single nanoparticles^[17,18].

Fig.4 shows the photoabsorption spectra obtained by the HWCS method for Ag, Al, Ni, Au, and Cr nanoparticles with two Na atoms near the nanoparticle's surface. In these spectra, the smaller radius of the nanoparticles results in more changes according to the presence of Na atoms. This means that smaller nanoparticles are more sensitive to the atomic subsystem. However, for each radius of the nanoparticles, the presence of Na atoms could change the photoabsorption spectrum. Note that the most changes in the photoabsorption spectrum belong to the energy range smaller than 4 eV. As can be seen from the comparison between Fig.3 and Fig.4, the photoabsorption spectrum is unchanged mainly due to the presence of the Na atoms, from 4 eV to 10 eV. However, for the energy ranges lower than 4 eV, the couples plasmon-enhanced absorptions may occur due to the strong interaction of the nanoparticle and Na atoms. This phenomenon is evident for the smaller nanoparticles, as shown in Fig.4. Although the enhanced photoabsorption of the structure can be seen from the simulation results, Na atoms do not change the photoabsorption spectra of the large nanoparticles, as shown in Fig.3 and Fig.4. This means that the smaller nanoparticles are more sensitive to the presence of Na atoms. Thus, they can be more precise in sensing applications.

Recent studies prove that pure classical calculations of SPR in the nanostructures show a superior sensitivity to the DNA molecules and nanoparticles^[1,4,19,20]. As in classical molecular dynamics, the interband plasmon in graphene nanopore can control the translocation speed of the DNA molecule through graphene nanopore^[21]. The plasmon-enhanced photoabsorption and coupled modes between the nanoparticles and atomic subsystems can be used for sequencing DNA molecules and sensing atomic-scale structures.

In summary, we utilized the HQCS to analyze photoabsorption spectra of metal nanoparticles. The hy-

brid method divides the structure of interest into quantum and classical subsystems. The quantum subsystem employs TDDFT to analyze the excited state of the atomic structure. Also, linear combinations of Lorentz



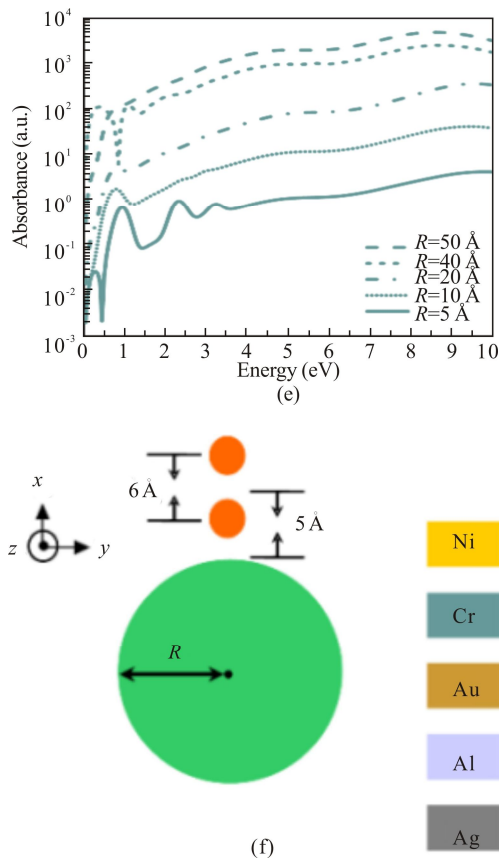


Fig.4 Photoabsorption spectra obtained from the HQCS method for (a) Ag, (b) Al, (c) Ni, (d) Au, and (e) Cr nanoparticles at the presence of two Na atoms (Effects of the size variations are shown for all nanoparticles. The photoabsorption quantities are shown on a logarithmic scale.)

oscillators represent material's permittivity for the classical subsystem. First, Lorentz parameters for Au, Ag, Al, Cr, and Ni permittivities are calculated. Photoabsorption spectra were obtained for a single metal nanoparticle with and without two Na atoms placed near the nanoparticles' surfaces. Au, Ag, Al, Cr, and Ni single nanoparticles show strong sensitivity to the presence of Na atoms. Our results prove that plasmon-enhanced coupled photoabsorption modes between a metal nanoparticle and atomic structures can be utilized in sensing devices.

Acknowledgment

Author thanks Tuomas Rossi for sharing valuable information on the GPAW code and calculation methods.

Statement and Declaration

The author declares that there are no conflicts of interest related to this article.

References

- [1] FARAMARZI V, AHMADI V, HEIDARI M, et al. Interband plasmon-enhanced optical absorption of DNA nucleobases through the graphene nanopore[J]. *Optics letters*, 2022, 47(1): 194-197.
- [2] COOMAR A, ARNTSEN C, LOPATA K A, et al. Near-field: a finite-difference time-dependent method for simulation of electrostatics on small scales[J]. *The journal of chemical physics*, 2011, 135(8): 084121.
- [3] GHORBANZADEH M, MORAVEJ-FARSHI M K, DARBARI S. Designing a plasmonic optophoresis system for trapping and simultaneous sorting/counting of micro-and nano-particles[J]. *Journal of lightwave technology*, 2015, 33(16): 3453-3460.
- [4] BELKIN M, CHAO S H, JONSSON M P, et al. Plasmonic nanopores for trapping, controlling displacement, and sequencing of DNA[J]. *ACS nano*, 2015, 9(11): 10598-10611.
- [5] YIN P, LIN Q, RUAN Y, et al. Investigation of multiple metal nanoparticles near-field coupling on the surface by discrete dipole approximation method[J]. *Optoelectronics letters*, 2021, 17(5): 257-261.
- [6] GAO Y, NEUHAUSER D. Dynamical quantum-electrodynamics embedding: combining time-dependent density functional theory and the near-field method[J]. *The journal of chemical physics*, 2012, 137(7): 074113.
- [7] SAKKO A, ROSSI T P, NEIMINEN R M. Dynamical coupling of plasmons and molecular excitations by hybrid quantum/classical calculations: time-domain approach[J]. *Journal of physics: condensed matter*, 2014, 26(31): 315013.
- [8] SUN D, DING Y Y, KONG L W, et al. First principles calculation of the electronic-optical properties of $\text{Cu}_2\text{MgSn} (\text{S}_x\text{Se}_{1-x})_4$ [J]. *Optoelectronics letters*, 2020, 16(1): 29-33.
- [9] DRAINE B T, FLATAU P J. User guide for the discrete dipole approximation code DDSCAT 7.0[EB/OL]. (2008-09-02) [2022-03-02]. <https://arxiv.org/abs/0809.0337>.
- [10] JOHNSON P B, CHRISTY R W. Optical constants of transition metals: Ti, V, Cr, Mn, Fe, Co, Ni, and Pd[J]. *Physical review B*, 1974, 9(12): 5056.
- [11] MCPEAK K M, JAYANTI S V, KRESS S J, et al. Plasmonic films can easily be better: rules and recipes[J]. *ACS photonics*, 2015, 2(3): 326-333.
- [12] MORTENSEN J J, HANSEN L B, JACOBSEN K W. Real-space grid implementation of the projector augmented wave method[J]. *Physical review B*, 2005, 71(3): 035109.
- [13] ENKOVAARA J, ROSTGAARD C, MORTENSEN J J, et al. Electronic structure calculations with GPAW: a real-space implementation of the projector augmented-wave method[J]. *Journal of physics: condensed matter*, 2010, 22(25): 253202.

- [14] WALTER M, HAKKINEN H, LEHTOVAARA L, et al. Time-dependent density-functional theory in the projector augmented-wave method[J]. *The journal of chemical physics*, 2008, 128(24): 244101.
- [15] BAHN S R, JACOBSEN K W. An object-oriented scripting interface to a legacy electronic structure code[J]. *Computing in science & engineering*, 2000, 4(3): 56-66.
- [16] HIBORN R C. Einstein coefficients, cross sections, f values, dipole moments, and all that[J]. *ArXiv preprint physics*, 2010: 0202029.
- [17] VAN DIJK M A, TCHEBOTAREVA A L, ORRIT M, et al. Absorption and scattering microscopy of single metal nanoparticles[J]. *Physical chemistry chemical physics*, 2006, 8(30): 3486-3495.
- [18] MUSKENS O L, DEL F N, VALLEE F. Femtosecond response of a single metal nanoparticle[J]. *Nano letters*, 2006, 6(3): 552-556.
- [19] ABASIFARD M, AHMADI V, FOTOUHI B, et al. DNA nucleobases sensing by localized plasmon resonances in graphene quantum dots with nanopore: a first principle approach[J]. *The journal of physical chemistry C*, 2019, 123(41): 25309-25319.
- [20] FOTOUHI B, AHMADI V, ABASIFARD M, et al. Petahertz-frequency plasmons in graphene nanopore and their application to nanoparticle sensing[J]. *Scientia iranica*, 2017, 24(3): 1669-1677.
- [21] FOTOUHI B, AHMADI V, ABASIFARD M. Controlling DNA translocation speed through graphene nanopore via plasmonic fields[J]. *Scientia iranica*, 2018, 25(3): 1849-1856.